

Demonstration of high efficiency elastocaloric cooling with large ΔT using NiTi wires

Jun Cui,^{1,2} Yiming Wu,¹ Jan Muehlbauer,³ Yunho Hwang,³ Reinhard Radermacher,³ Sean Fackler,¹ Manfred Wuttig,¹ and Ichiro Takeuchi^{1,a)}

¹Department of Materials Science & Engineering, University of Maryland, College Park, Maryland 20742, USA

²Energy and Environment Directorate, Pacific Northwest National Lab, Richland, Washington 99354, USA

³Department of Mechanical Engineering and Center for Environmental Energy Engineering, University of Maryland, College Park, Maryland 20742, USA

(Received 14 May 2012; accepted 2 August 2012; published online 17 August 2012)

Vapor compression (VC) is by far the most dominant technology for meeting all cooling and refrigeration needs around the world. It is a mature technology with the efficiency of modern compressors approaching the theoretical limit, but its environmental footprint remains a global problem. VC refrigerants such as hydrochlorofluorocarbons (HCFCs) and hydrofluorocarbons (HFCs) are a significant source of green house gas emissions, and their global warming potential (GWP) is as high as 1000 times that of CO₂ [Buildings Energy Data Book (Building Technologies Program, Department of Energy, 2009)]. There is an urgent need to develop an alternative high-efficiency cooling technology that is affordable and environmentally friendly [A. D. Little, Report For Office of Building Technology State and Community Programs, Department of Energy, 2001]. Here, we demonstrate that elastocaloric cooling (EC), a type of solid-state cooling mechanism based on the latent heat of reversible martensitic transformation, can have the coefficient of performance as high as ≈ 11 , with a directly measured ΔT of 17 °C. The solid-state refrigerant of EC completely eliminates the use of any GWP refrigerants including HCFCs/HFCs. © 2012 American Institute of Physics. [<http://dx.doi.org/10.1063/1.4746257>]

The elastocaloric cooling (EC) is directly related to the well-known phenomenon of reversible solid-to-solid martensitic phase transformation.¹⁻⁴ In many ways, the EC concept is analogous to the conventional vapor compression (VC) cycle technology because it uses stress to induce phase transformation and utilizes latent heat to achieve cooling. The difference lies in the form of the refrigerant. It is liquid/vapor for vapor compression and solid/solid for elastocaloric cooling.

The elastocaloric cooling effect is best illustrated using a wire made of a superelastic shape memory alloy. When stressed with two hands, the wire is forced to transform to a martensite phase releasing latent heat. For some alloys, the released heat can be as high as 20 J/g.⁵ This amount of heat suffices to leave a burning sensation to the skin. Upon stress removal, the wire transforms back to its parent phase absorbing similar amount of heat resulting now in icy-cold sensation to the touch. Figure 1 (and the supplementary movie file) shows thermal images of a 0.5 mm diameter NiTi wire in air when tensile force of ~ 67 Newtons is applied (a) and subsequently removed (b).

The key parameters of cooling technologies include the adiabatic temperature change, ΔT , work per unit volume, and the coefficient of performance (COP). We have carried out a set of experiments to quantitatively evaluate the elastocaloric cooling effect of the NiTi alloy. A set of elastocaloric wires NiTi (equiatomic percent of nickel and titanium, manufactured by Nitinol Devices and Components, Inc) were

stretched and compressed by a material testing system, and the temperature changes of the wires were recorded. The measurements of wires were carried out in air without any thermal insulation. The wires with different diameters were machined from the same alloy composition of NiTi. For each diameter, the measurements were repeated using three different samples cut (typical length ~ 178 cm for tension and 0.5 cm or 1 cm for compression) from different sections of the same wire spool. All wires are stressed till the theoretical strain limit is reached (8.5% for tension and 6.0% for compression). At this point, the temperature of the wire rises due to latent heat release triggered by stress induced phase transformation. The stress is then held for 300 s to let the wire reach thermal equilibrium with air and the temperature to reach back the room temperature. Then, the stress is unloaded at a strain rate of 100 mm/min, which causes a sudden drop of the wire's temperature. A K-type thermocouple is placed at the mid point of the wire to monitor the non-adiabatic temperature change during the loading, holding, and unloading processes.

Figure 2 plots the temperature and the tensile stress as function of time for a NiTi wire with 3 mm diameter. Upon loading, the temperature of the wire rapidly rises by 22 °C, followed by an additional increase of 2 °C in the subsequent 10 s reaching a maximum $\Delta T = 25.5$ °C. The temperature then begins to drop gradually to room temperature due to the absence of thermal insulation. Upon unloading, the wire temperature rapidly decreases by about 12 °C, followed by an additional drop of 5 °C in the following 10 s reaching a maximum $\Delta T = 17$ °C. The difference between the $\Delta T_{\text{loading}}$ ($= 25.5$ °C) and $\Delta T_{\text{unloading}}$ ($= 17$ °C) is 8.5 °C which we

^{a)} Author to whom correspondence should be addressed. Electronic mail: takeuchi@umd.edu.

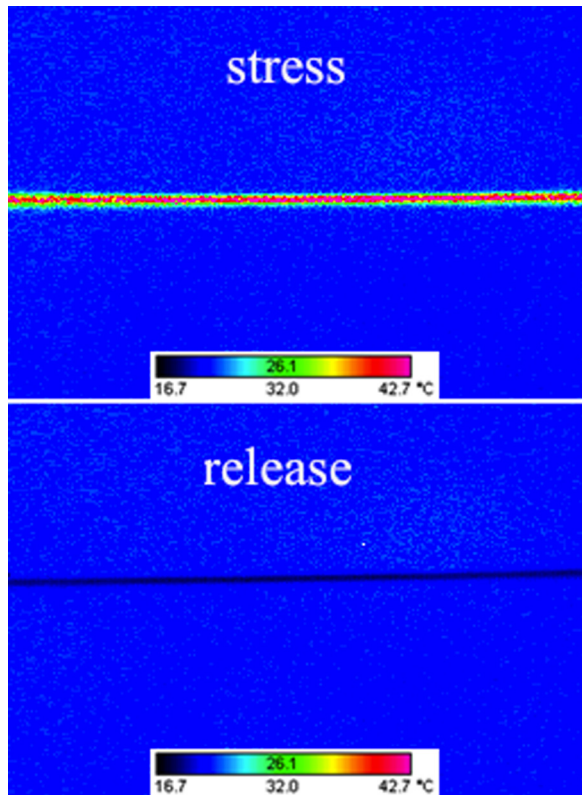


FIG. 1. Thermal images of a nitinol wire being stressed and subsequently relaxed.

attribute to heating caused by rapid loading, which is due to slip and other dissipating mechanisms as commonly observed in metallic compounds.

The measured non-adiabatic temperature changes of the wires with different diameters can be used to derive the adiabatic temperature change, $\Delta T_{adiabatic}$, which can be compared to the theoretical maximum value obtained using the relation $\Delta T_{theory} = L/C_p$, where L and C_p denote the latent heat and the heat capacity, respectively. Figure 3 summarizes the measured $\Delta T_{unloading}$ of the wires with different diameters,

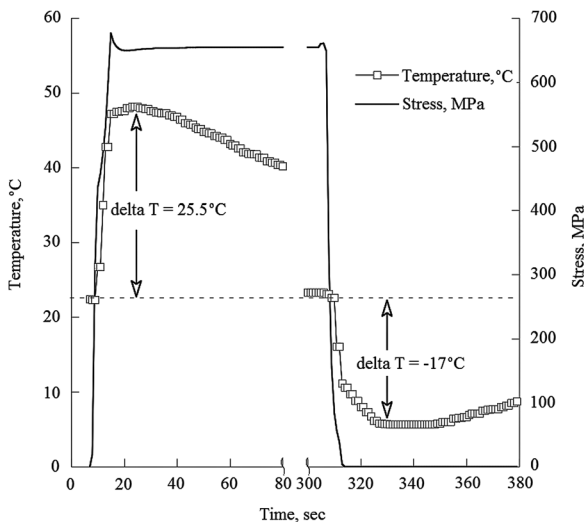


FIG. 2. Temperature and Stress curves as function of time for a NiTi wire with 3 mm diameter under tensile test. The wire temperature increases 25.5 °C spontaneously upon loading, and decreases -17 °C within about 10 s of loading/unloading.

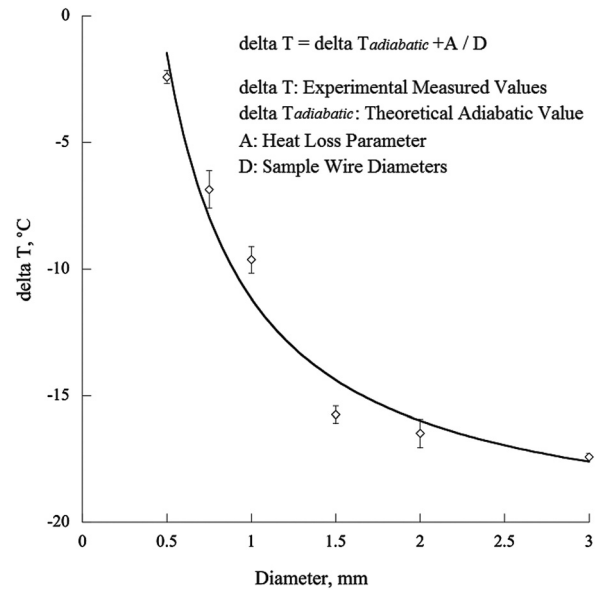


FIG. 3. The temperature change of NiTi wires with various diameters under tensile tests. The temperature changes were measured when the applied stress is removed. The fitting curve indicates the theoretical $\Delta T_{adiabatic}$ of -20.8 °C.

and the fitting curve using an equation, which takes into account the fact that temperature loss is inversely proportional to the surface area of the wire. The fitting parameters show that the extrapolated $|\Delta T_{adiabatic}| = 20.8^\circ\text{C}$. This number is in good agreement with the theoretical maximum value, $\Delta T_{theory} = 21.8^\circ\text{C}$, using the latent heat (12 kJ/kg) and the heat capacity (0.55 kJ/kg-°C) measured by differential thermal calorimetry (DSC) for a 3 mm wire. The corresponding work per unit volume is 78 MJ/m³, which is six times that of a state-of-the-art VC refrigerant (12.9 MJ/m³, calculated using latent enthalpy of 195 kJ/kg at 20 °C and the applied stress of 1.4 MPa, with the density of its saturated vapor of 66 kg/m³).⁶

Figure 4 shows the stress-strain curves for a 3 mm diameter NiTi wire under tension and compression. The COP is obtained by dividing the latent heat by the mechanical

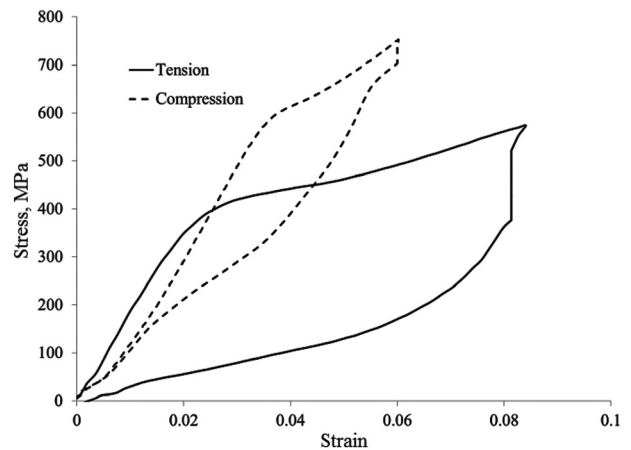


FIG. 4. Stress strain curves for two pieces of 3 mm diameter wires during the tension (178 cm long sample) and compression tests (1 cm long sample). The areas underneath the loading curve for tension and compression are about 29 and 25.6 MJ/m³, respectively; the areas enveloped by the loading/unloading curve are about 21.1 and 6.6 MJ/m³, respectively.

energy applied to the wire to induce the martensitic phase transformation. The applied mechanical energy is calculated by integrating the area enclosed by the stress-strain curve. For tension, the area enclosed by the loading and the horizontal axis is 29.0 MJ/m^3 , and the area enclosed by loading and unloading curves is 21.1 MJ/m^3 . The temperature change observed during the cycle is between the lowest point of 5°C after unloading to the highest point of 47.5°C after loading (From 2). For compression, the area enclosed by the loading and the horizontal axis is 25.6 MJ/m^3 , and the area enclosed by loading and unloading curves is 6.6 MJ/m^3 . The temperature change observed for compression is between the lowest point of 9°C after unloading and the highest point of 29°C after loading (not shown). With the density of NiTi of about 6500 kg/m^3 , the COPs for tension and compression are 2.7 and 3.05 using the area between the loading curve and the horizontal axis, respectively, which are 41.3% and 21.6% of the theoretical Carnot cycle COP values ($T_c/(T_h-T_c)$) where the lowest/highest temperature observed in the cycle is used as T_c/T_h . These values are assuming that the unloading energy is not recoverable. However, if we have a cooling system that can utilize the unloading work, the COPs are 3.7 and 11.8 calculated using the areas enclosed by the loading and the unloading curves, which correspond to 56.5% and 83.7% of the Carnot cycle values for tension and compression, respectively.

Several factors contribute to the drastic difference in COP values obtained from compression and tension cycles. First, the compression stress strain curve does not exhibit any stress plateau that is typical for a tension test. Second, it requires much less strain to fully transform the material during the compression test than it is required for tension. But, more importantly, it is the steep unloading compression curve that significantly increases the recoverable unloading energy from the compression cycle.

Table I compares the ratio of the obtained COP to that of the theoretical Carnot cycle ($\text{COP}_{\text{Carnot}}$) in the same temperature range for various alternative cooling technologies. We take this ratio to be the ultimate measure of efficiency. The electrocaloric effect is not yet commercially exploited, as the current demonstrated effect is not yet sufficient for practical applications due to the low heat conductivity of the working materials and limitations of their cooling capacity.^{7,8} Magnetocaloric (MC) refrigeration relies on the magnetocaloric effect, where a reversible temperature change is caused by the application and removal of a magnetic field. Efforts to commercialize current magnetic refrigeration technology have

been ineffectual due to the high cost implicated by the fundamental requirement of large quantity of rare-earth elements for the magnets. One feasibility study has concluded that a minimum of $10\times$ reduction in cost is necessary for MC to reach market entry point.⁹ Recently, a barocaloric effect which combines MC and elastocaloric cooling was reported.¹⁰ Thermoacoustic refrigeration relies on the ideal gas law, where high amplitude sound waves are applied to a pressurized gas to pump heat. One of the most efficient thermoacoustic devices built by Garrett *et al.* has the overall system efficiency of about 19%. Despite significant progress achieved in the past decades, the commercial viability of the current thermoacoustic technology remains low. The maximum efficiency of the Peltier refrigerators based on the thermoelectric effect is about $5\%\sim 10\%$ ultimately limiting its application to small scale systems, and their overall impact on mitigating the modern energy shortage and global warming is small.

The measured COP of the elastocaloric cooling on NiTi alloys is the second highest among all the solid-state based refrigeration technologies. Even though this value is comparable to that of a VC cycle process, the complete elimination of the refrigerants with global warming potential (GWP) and the low system cost implied by the simplicity of the operation principle make elastocaloric cooling technology an attractive alternative to the VC technology. In addition, there are several approaches to further improve the efficiency of elastocaloric coolers. One is through materials optimization. The materials used in the present experiments (NiTi wires) were chosen because of their availability. Literature shows that through chemical substitution and heat treatment, the latent heat of martensitic transformation can be increased to be as high as 31 J/g .¹¹ The other approach is through proper system design that allows the utilization of recovered work. The calculated COP of 11.8 assumes that the cooling system can effectively use the unloading energy to run the cycle.

One potential shortcoming of elastocaloric cooling based on shape memory alloys is their fatigue life. For an elastocaloric system operating at 1 Hz, to reach a typical life of 10 years (assuming operation of 6 months per year and 12 h per day), the refrigerant has to undergo stress-induced phase transformation 78 million times. For any alloy to survive this many loading cycles, the material must be able to resist crack propagation or the pre-existing cracks must be below a critical size. For the material used in the experiments, the critical size a is calculated to be $14 \mu\text{m}$ using the expression $a = (K_{IC}/\sigma)^2/\pi$, where the critical stress

TABLE I. Comparison of different cooling technologies.

Technology	Maturity	Principle	COP/ $\text{COP}_{\text{Carnot}}$	Environmental impact	Cost	References
Vapor compression	Commercial	Vaporization latent heat	Up to 60%	High	Low	15
Thermoelectric	Commercial	Peltier effect	Up to 10%	Low	Med	16–18
Thermoacoustic	System under development	Ideal gas law	Up to 40%	Low	Med	19–21
Magnetocaloric	Technology under development	Magnetocaloric effect	Up to 70% (Ref. 22)	Low	High	23–25
Elastocaloric	Technology concept formulated	Martensitic phase transformation latent heat	Up to 83.7% (Ref. 26)	Low	Low	3 and 27, this work
Electrocaloric	Basic principles observed	Electrocaloric effect	—	Low	High	7, 8, and 28

intensity factor is given by $K_{IC} = 2 \text{ MPa(m)}^{0.5}$ for the NiTi alloy and the minimum required stress is $\sigma = 300 \text{ MPa}$.¹² Meeting this requirement is very challenging but feasible. Actually, it is a common practice in the medical stent industry to consistently produce a NiTi stent with the size of pre-existing cracks less than $10 \mu\text{m}$. On the other hand, if compression is used instead of tension, cracks will have little chance to grow and a much longer life span can be expected even for a material with relatively large cracks. We have recently demonstrated substantial enhancement in functional fatigue properties of shape memory alloys through lattice-constant engineering as dictated by the non-linear theory of martensites.^{13,14} This technique is naturally expected to play an important role in selecting the optimum material composition for elastocaloric cooling in the future. We also note that an intriguing alternative to shape memory alloys as an active material for elastocaloric cooling is polymers with latent heat in their stretch transformation.

This work was supported by DOE ARPA-E DEAR0000131, PNNL TMS 2010, and ARO W911NF-07-1-0410.

- ¹J. Quarini and A. Prince, *Prog. Inst. Mech. Eng., Part C: J. Mech. Eng. Sci.* **218**, 1175–1178 (2004).
- ²E. Bonnot, R. Romero, L. Manosa, E. Vives, and A. Planes, *Phys. Rev. Lett.* **100**, 125901 (2008).
- ³P. O. Castillo-Villa, D. E. Soto-Parra, J. A. Matutes-Aquino, R. A. Ochoa-Gamboa, A. Planes, L. Manosa, D. Gonzalez-Alonso, M. Stipcich, R. Romero, D. Rios-Jara, and H. Flores-Zuniga, *Phys. Rev. B* **83**, 174109 (2011).
- ⁴L. Manosa, A. Planes, E. Vives, E. Bonnot, and R. Romero, *Funct. Mater. Lett.* **V2**(n2), 73–78 (2009).
- ⁵J. A. Shaw, C. B. Churchill, and M. A. Iadicola, *Exp. Tech.* **32**(5), 55–62 (2008).
- ⁶DuPont Suva refrigerants, Technical information, ART-38 (2004).

- ⁷A. S. Mischenko, Q. Zhang, J. F. Scott, R. W. Whatmore, and N. D. Mathur, *Science* **311**(5765), 1270–1271 (2006).
- ⁸B. Neese, B. Chu, S.-G. Lu, Y. Wang, E. Furman, and Q.-M. Zhang, *Science* **321**(5890), 821 (2008).
- ⁹F. Johnson, private research communications (2011).
- ¹⁰L. Manosa, D. Gonzalez-Alonso, A. Planes, E. Bonnot, M. Barrio, J.-L. Tamarit, S. Aksoy, and M. Acet, *Nature Mater.* **9**, 478–481 (2010).
- ¹¹J. Otubo, O. D. Rigo, A. A. Coelho, C. M. Neto, and P. R. Mei, *Mater. Sci. Eng. A* **481–482**, 639–642 (2008).
- ¹²A. L. McKelvey and R. O. Ritchie, *J. Biomed. Mater. Res.* **47**(3), 301–308 (1999).
- ¹³J. Cui, Y. S. Chu, O. O. Famodu, Y. Furuya, J. Hattrick-Simpers, R. D. James, A. Ludwig, S. Thienhaus, M. Wuttig, Z. Zhang, and I. Takeuchi, *Nature Mater.* **5**, 286–290 (2006).
- ¹⁴R. Zarnetta, R. Takahashi, M. L. Young, A. Savan, Y. Furuya, S. Thienhaus, B. Maass, M. Rahim, J. Frenzel, H. Brunken, Y. S. Chu, V. Srivastava, R. D. James, I. Takeuchi, G. Egeler, and A. Ludwig, *Adv. Funct. Mater.* **20**, 1–7 (2010).
- ¹⁵The Canadian Renewable Energy Network publication “Commercial Earth Energy System” (CANMET Energy Technology Centre-Varennes, CANETA Research and TECHNOSIM Consulting Group For Renewable and Electrical Energy Division, Natural Resources of Canada, ISBN 0-662-32808-6, Cat. No. M92-252/2002E, 2002).
- ¹⁶TE Technology, Inc., Technical Information (2010).
- ¹⁷D. S. Kim and C. A. Ferreira, *Int. J. Refrig.* **31**, 3–15 (2008).
- ¹⁸G. J. Snyder and T. S. Ursell, *Phys. Rev. Lett.* **91**(14), 148301 (2003).
- ¹⁹S. Backhaus and G. W. Swift, *Nature (London)* **399**, 335–338 (1999).
- ²⁰S. L. Garrett, *Am. J. Phys.* **72**, 11–17 (2004).
- ²¹W. V. Slaton, R. Raspet, C. J. Hickey, and R. A. Hiller, *J. Acoust. Soc. Am.* **112**(4), 1423–1430 (2002).
- ²²Calculated by dividing measured COP by Carnot cycle COP for the same temperature range.
- ²³K. A. Gschneidner and V. K. Pecharsky, *Annu. Rev. Mater. Sci.* **30**, 387–429 (2000).
- ²⁴J. L. Hall and J. A. Barclay, *Adv. Cryog. Eng.* **43**, 1719–1728 (1998).
- ²⁵K. A. Gschneidner, V. K. Pecharsky, and C. B. Zimm, in *Proceedings of the 50th Annu. Inter. Appl. Tech.* (1999), pp. 144–154.
- ²⁶Estimated based on materials performance instead of system performance.
- ²⁷L. Manosa, A. Planes, E. Vives, E. Bonnot, and R. Romero, *Funct. Mater. Lett.* **V2**(n2), 73–78 (2009).
- ²⁸S. G. Lu, B. Rozic, Q. M. Zhang, Z. Kutnjak, R. Pirc, M. Lin, X. Li, and L. Gorny, *Appl. Phys. Lett.* **97**, 202901 (2010).